

# Preparation and catalytic performance of mesostructured aluminosilicate nano-particles with wormhole-like framework structure

Shangru Zhai<sup>a,\*</sup>, Ye Zhang<sup>a</sup>, Xi'e Shi<sup>a,b</sup>, Dong Wu<sup>a</sup>, Yuhua Sun<sup>a</sup>, Yongkui Shan<sup>b</sup>, and Mingyuan He<sup>b</sup>

<sup>a</sup>State Key Laboratory of Coal Conversion, Institute of Coal Chemistry, Chinese Academy of Sciences, Taiyuan 030001, P.R. China

<sup>b</sup>Department of Chemistry, East China Normal University, Shanghai 200063, P.R. China

Received 10 October 2003; accepted 13 January 2004

A facile two-step sol-gel method has been developed for the preparation of mesostructured aluminosilicate nano-particles (Si/Al = 7.5) with wormhole-like but uniform pore structures and highly catalytic activities towards bulky hydrocarbon cracking. It is desirable that, as this synthesis takes place in the absence of alkali cations, the mesoporous nano-particulate material is directly obtained in the acid form, making a subsequent ion-exchange and calcination treatment superfluous.

**KEY WORDS:** sol-gel; mesostructured; nano-particle; synthesis; catalysis.

## 1. Introduction

The fabrication of nano-scale devices and the preparation of structures with ordered mesoporosity are two hotspot of current research in materials chemistry. It is well known that materials with length scales on the order of 1–100 nm possessing interesting and potentially useful catalytic, magnetic, optical and semi-conducting properties for technological and biomedical applications [1]. Likewise, ordered mesostructured materials, such as the M41S family of silicas, are an important new class of inorganic oxides with enormous potential in molecular sieving, catalysis (e.g., for large molecule transformations), and adsorption processes [2]. So, it is scientific interesting to combine the methods of nano-particles synthesis with those leading to the templating of open framework mesoporous materials to produce nano-sized objects with both external (surface) and internal (bulk) functionalization. In this regard, several recent reports described the formation of mesostructured nano-particles [3–8]. However, most of published studies on mesostructured nano-particles have mainly focused on pure silica or organically modified hexagonally ordered MCM-41 [3–6]. This is primarily due to the difficulty of fabricating mesostructured nano-particles, i.e., these nano-sized objects are not obtainable under conventional synthesis conditions, usually need specialized techniques [3–5,8].

Recently, it has been shown that mesostructured aluminosilicate nano-particles can be prepared by employing co-templates method [7]. This approach is based on the use of expensive TEAOH as the template of Beta seeds for the construction of pore walls and starch as the mesostructure-directing agent. However,

the pore sizes in these particles are relatively broad (9–20 nm) compared with that of conventional mesoporous materials and the synthesis method involves several tedious steps at elevated temperatures.

We have recently reported the preparation of wormhole-like AIMSU-X with high activity in bulky hydrocarbon cracking [9]. In the present work, we present another route to the production of highly catalytic mesoporous aluminosilicate nano-particles with particle size less than 100 nm, and experimental results show that the material with wormlike but uniform mesostructured interiors can be routinely obtained by a simple sol-gel method at low temperature.

## 2. Experimental

### 2.1. Synthesis

Mesostructured aluminosilicate nano-particles were prepared from tetraethylorthosilicate (TEOS) as the silica source and aluminum nitrate ( $\text{Al}(\text{NO}_3)_3 \cdot 9\text{H}_2\text{O}$ ) served as the aluminum ion precursor with cetyltrimethylammonium bromide (CTAB) as template. In a typical synthesis, two solutions were prepared under gentle stirring. Solution A, formed by 16.62 g of TEOS [purity, 99.9999%] and 35.7 ml of ethyl alcohol [purity, 99.7%]; and solution B, made up of 6.83 g CTAB [purity, 99.0%], 3.71 g aluminum nitrate [purity, 99.0%] and 54 ml distilled water. Once these solutions were homogenized, solution A was added to solution B and the obtained mixture was sealed and stirred for 4–6 h. After then 50 ml ammonia water [wt, 25–28%] was quickly poured into the above mixture under vigorous stirring to give a gel of molar ratio  $\text{TEOS}:0.133\text{-Al}(\text{NO}_3)_3 \cdot 9\text{H}_2\text{O}:0.25\text{ CTAB}:8\text{ C}_2\text{H}_5\text{OH}:10\text{ NH}_4\text{OH}$ :

\* To whom correspondence should be addressed.

40 H<sub>2</sub>O. After continuous stirring for 2 h at room temperature, the resulting gel was placed in a oven and heated at 50–65 °C for 72 h. The solid product was filtered, washed thoroughly with distilled water, dried and calcined in air at 650 °C for 6 h to remove the templates occluded in the pores. It should be noted here that, since the synthesis takes place in the absence of alkali metal cations (such as Na<sup>+</sup>), the aluminosilicate nano-particles were directly obtained in the acid form, making subsequent ion-exchange and activation procedures superfluous.

## 2.2. Measurement

XRD patterns were recorded at room temperature on a Rigaku D Max III VC instrument with Ni filtered Cu K<sub>α</sub> radiation ( $\lambda = 1.5404 \text{ \AA}$ ), in the  $2\theta$  range of 1°–6° at a scan rate of 1°/min. HRTEM images were taken on a Jeol Model 1200 EX instrument operated at an accelerating voltage of 200 kV. The specific surface area of the samples was determined by the BET method using N<sub>2</sub> adsorption measured with a Tristar 3000 analyzer. Prior to the adsorption, the samples were degassed at 150 °C for 6 h at 10<sup>−4</sup> Torr. The <sup>27</sup>Al MAS NMR experiments were performed on a Bruker MSL 300 spectrometer, in a 7 mm zirconia rotor at 4.0 kHz and 11.7 Tesla. Chemical shifts were measured with respect to Al(H<sub>2</sub>O)<sub>6</sub><sup>3+</sup> as the reference. NH<sub>3</sub>-TPD was performed on 200 mg of catalyst with nitrogen (40 ml/min) as the carrier gas and a thermoconductor as the detector. NH<sub>3</sub>-TPD profile was obtained in the range of 120–600 °C with a heating rate of 10 °C/min. IR-pyridine adsorption was obtained on Impact 410, Nicolet spectrometer. The self-supporting wafers about 5 mg/cm<sup>2</sup> were evacuated *in situ* in an IR cell under vacuum (10<sup>−5</sup> Torr) at 400 °C for 4 h and cooled to room temperature, then pyridine molecules were exposed to the disks. After adsorption at room temperature for 0.5 h and evacuation at 150 for 0.5 h, the spectra were recorded.

## 2.3. Catalytic test

Catalytic cracking of 1,3,5-triisopropylbenzene was carried out at 250–340 °C by pulse method to evaluate catalytic performance of the sample. In each run, 60 mg of catalyst was used, the pulse injection of the reactant was 0.2  $\mu$ l, and nitrogen was used as carrier gas at a flowing rate of 50 ml/min. The reaction products were analyzed using GC-9A gas chromatograph (Shimadzu Co.) equipped with FID and a high resolution Chrom-Workstation Data Set.

Blank experiments were also carried out under the same reaction conditions but substitute pure SiO<sub>2</sub> (quartz) for the catalyst in the reactor. No distinguishable cracking products were observed in these blank experiments, even at the highest temperature tested in this work.

## 3. Results and discussion

Figure 1 shows XRD pattern of the calcined aluminosilicate nano-particles. As shown, a broad reflection in the  $2\theta$  range of 1°–3° is represented. This has also been observed by Bagshaw [10], and ascribed to either a small-size effect of a hexagonal material (HMS) or the presence of three-dimensional (3D) wormhole-like pore structures (MSU).

Indeed transmission electron microscopy (TEM) image of the calcined product (figure 2A) reveals that the material is comprised almost entirely of discrete and regular nano-particles with slightly well-defined edges and grain sizes less than 100 nm. Furthermore, a high magnification image shows 3D full-disordered but uniform mesopores (see figure 2B), clearly indicating these aluminosilicate nano-particles have disordered framework pores similar to that for KIT-1 material

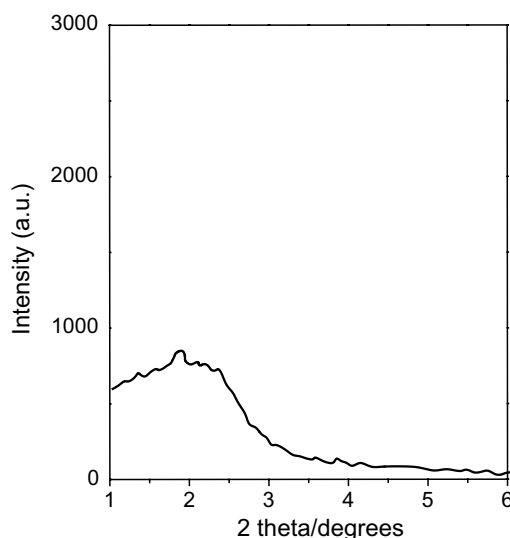


Figure 1. XRD pattern of the calcined mesostructured nano-particles.

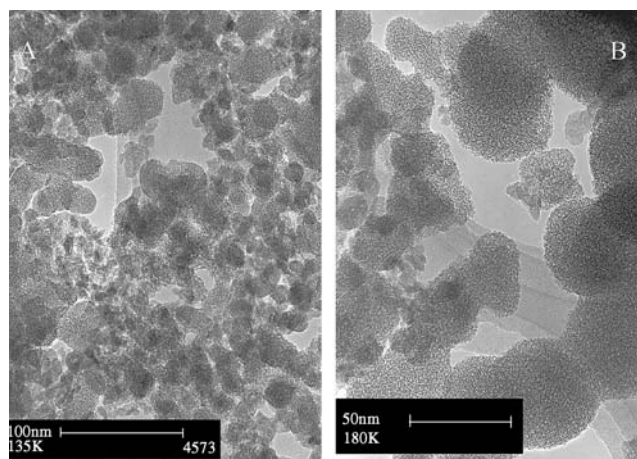


Figure 2. Low (A) and high magnification (B) TEM images of the calcined nano-particles.

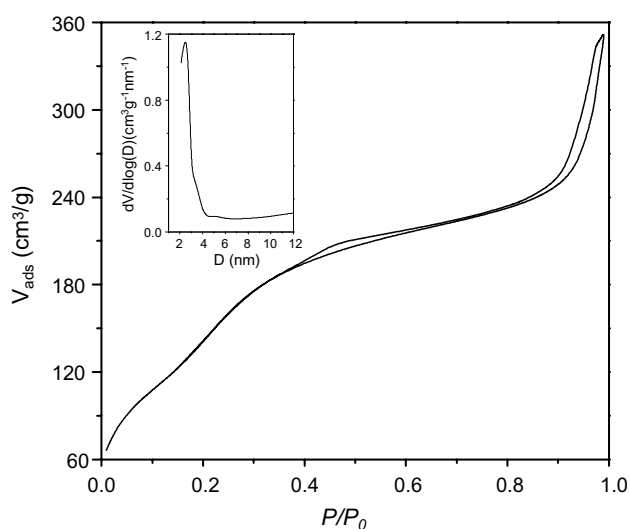


Figure 3. Nitrogen adsorption isotherm and pore size distribution (insert) of the mesoporous aluminosilicate nano-particles.

synthesized by hydrothermal method in the presence of various organic polyacids [11].

The nitrogen adsorption isotherm and pore size distribution for the nanoparticles are shown in figure 3. The product exhibits a complex isotherm not only with a definite step in the relative pressure range of 0.15–0.3, typical of capillary condensation of nitrogen into the uniform framework mesopores, but also with another more observed step in the range of 0.8–1.0, which may be due to the filling of larger mesopores caused from the void space among the nano-sized particles. Correspondingly, the BJH pore size distribution calculated from desorption branch of the isotherm for the nano-particles shows a sharp distribution around 2.49 nm (see figure 3 insert), which is much more uniform than that for reported aluminosilicate nano-particles [7,8], and is in agreement with the pore size estimated from the TEM analysis (figure 1B). Furthermore, a high BET surface area of  $537 \text{ m}^2 \text{ g}^{-1}$  and a single point ( $P/P_0 = 0.971$ ) total adsorption pore volume of  $0.465 \text{ cm}^3 \text{ g}^{-1}$  are observed for the mesoporous nano-particles.

Figure 4 illustrates the  $^{27}\text{Al}$  MAS NMR spectra of the as-synthesized and calcined nano-particles. Noticeably, all the aluminum in the as-synthesized form is incorporated into the tetrahedral positions of the pore walls, even with a Si/Al ratio as low as 7.5. This fact indicates that the quickly addition of ammonia water played a key role, as it allows us to accelerate the synthesis and favors the incorporation of aluminum into the framework. However, the  $^{27}\text{Al}$  MAS NMR spectrum for the calcined nano-particles shows the appearance of three distinct signals center at  $-5.6$ ,  $21$  and  $53 \text{ ppm}$ , respectively. The high-field signal corresponds to octahedral aluminum, and that at  $53 \text{ ppm}$  is assigned to tetrahedral aluminum. Of interest is the presence of the line at  $21 \text{ ppm}$ , which can be assigned to five-coordi-

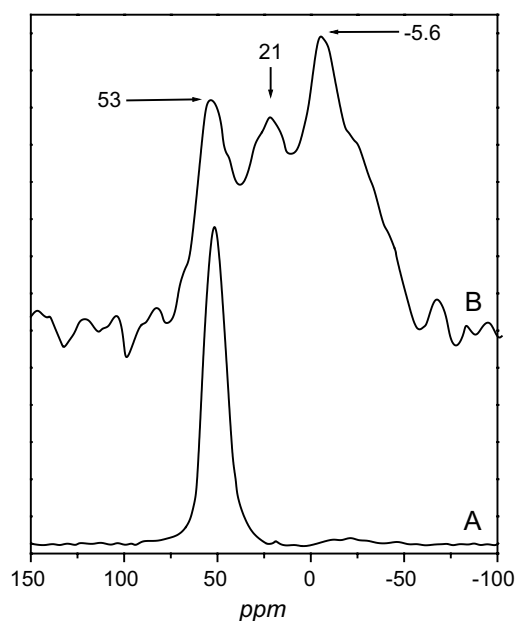


Figure 4.  $^{27}\text{Al}$  MAS NMR spectra of the as-synthesized (A) and calcined (B) aluminosilicate nano-particles.

nated aluminum or, alternatively, aluminum in highly distorted tetrahedral sites. Although the five-coordinated aluminum has been identified under certain synthesis conditions [12], it can not generally be observed in calcined aluminum-rich AIMCM-41 materials even for very low Si/Al ratios [13]. It should be also noted that aluminum expulsion phenomenon has been commonly observed for many Al-containing mesoporous materials after calcination, regardless of the synthesis conditions [14,15].

Figure 5 displays *in situ* FTIR spectrum of pyridine adsorption on the surface of nano-particles after it has been degassed at  $150^\circ\text{C}$  for 0.5 h. It can be clearly seen that it exhibits bands at the  $1460$ ,  $1490$ ,  $1550$  and  $1620 \text{ cm}^{-1}$ . According to a recent study [16], the bands at  $1460$  and  $1620 \text{ cm}^{-1}$  are attributed to Lewis acid sites, the band at  $1550 \text{ cm}^{-1}$  is assigned to Brönsted acid centers and the band at  $1490 \text{ cm}^{-1}$  is ascribed to a combinational signal associated with both Lewis and Brönsted acid sites. Notably, intensity of the band  $1460 \text{ cm}^{-1}$  is much stronger than that of  $1550 \text{ cm}^{-1}$ , strongly indicating the nano-particles have many more exposed Lewis centers than Brönsted acid sites, which is well consistent with the  $^{27}\text{Al}$  MAS NMR observation, i.e., large part of Al atoms dealuminate from the framework forming non-structural Al species after calcination.

Another interesting fact is that these nano-particles do not need to be treated by ion-exchange to turn them into acid form. This is a great advantage, as it eliminates the necessity for an additional calcination stage after the ion-exchange that could cause an undesirable further dealumination. Figure 6 illustrates  $\text{NH}_3$ -TPD profile of

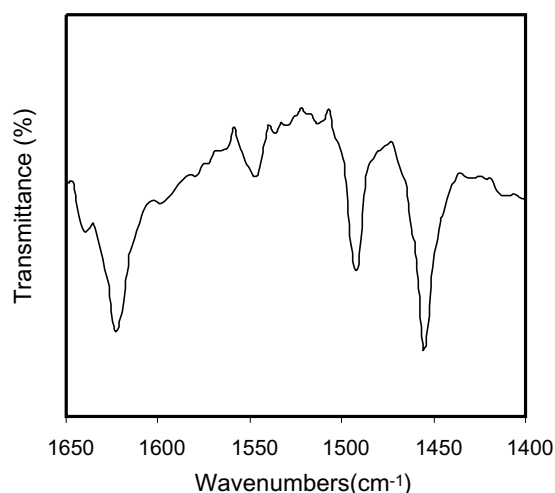


Figure 5. FTIR spectrum of pyridine adsorbed on the aluminosilicate nano-particles after they have been degassed under vacuum at 150 °C for 0.5 h.

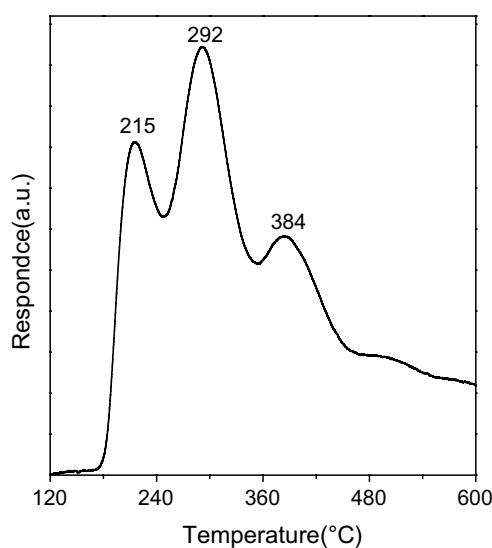


Figure 6. NH<sub>3</sub>-TPD profile of the calcined aluminosilicate nano-particles.

the calcined nano-particles. Obviously, three desorption peaks at 215, 292 and 384 °C that may cause from weak, medium and strong acid sites can be observed, respectively. Whereas the lower temperature peak of 215 °C can be attributed to physisorbed and weakly bonded ammonia molecules [17], the second and third peaks are ascribed to ammonia molecules desorbed from medium and strong acid sites [14,18], respectively. The “medium” to “weak” to “strong” acid sites ratio determined from the corresponding TPD peak areas is about 1.0:0.77:0.32. It is therefore concluded that most of acid sites presented on the surface of these nano-particles are medium despite there is small amount of strong acid sites.

Generally speaking, the cracking of 1,3,5-triisopropylbenzene with three isopropyl units needs the catalysts with medium acidity [19]. Table 1 lists the catalytic data for 1,3,5-triisopropylbenzene cracking over the aluminosilicate nano-particles with medium acidity. Obviously, the nano-particulate material exhibits very high conversion capability, giving 100% even at the lowest 250 °C. This may be related to, on the one hand, the small particle size and wormlike pore structures they

have, as it is well established that for catalysis, small particle size and 3D pore channels allowing easy access of the reactant molecules to the acid sites and diffusion of product molecules out of the pores [7,20,21]; on the other hand, the low Si/Al ratio (~9.8 after calcination) in the nano-particles. Furthermore, the product distribution over the material varies remarkably with reaction temperatures, obviously indicating that cracking extent of the reactant becomes deeper with higher reaction temperature used.

We have presented here what we believe to be a simple and straightforward method for the preparation of mesostructured aluminosilicate nano-particles. The main feature of this sol-gel approach lies in the capability to discriminate the assembly step from the hydrolysis step. To this purpose we applied the sol-gel method involved two steps that utilizes a mild acid medium (pH ca. 2.73) results from the hydrolysis of Al<sup>3+</sup>, in which a stable colorless micro-emulsion containing all reactants is obtained. Hence, whatever the initial homogeneity of the CTAB-TEOS-aluminum species-C<sub>2</sub>H<sub>5</sub>OH mixture, the homogeneity at the molecular level is always attained before the reaction starts.

Table 1  
Catalytic activities in 1,3,5-triisopropylbenzene cracking of the aluminosilicate nano-particles at different temperatures

Temperature	Conversion (mol%) <sup>a</sup>	Selectivity (%)				
		Propylene	Benzene	Cumene	<i>m</i> -Diisopropylbenzene	<i>p</i> -Diisopropylbenzene
250	100	35.95	0.61	34.29	21.13	8.02
280	100	40.87	2.05	42.72	10.43	3.93
310	100	42.90	4.53	45.14	5.22	2.20
340	100	46.74	10.43	41.27	1.56	–

Note: Here, (–) means the product was undetectable.

<sup>a</sup> Conversions presented here were the second pulse.

Therefore, the quick addition of ammonia water leads to the rapid nucleation and aggregation process and therefore the formation of mesostructured aluminosilicate nano-particles.

#### 4. Conclusions

In summary, a nano-sized mesostructured Al-containing material with 3D wormhole-like but uniform mesopores has been facilely synthesized via sol-gel method at low temperature. Catalytic data in 1,3,5-triisopropylbenzene cracking show that the conversion over the nano-particles is amounted to 100% even at 250 °C, suggesting that the mesostructured material may be a helpful catalyst for catalytic cracking of bulky residues especially when high-temperature reaction condition is required.

#### Acknowledgment

This work was funded by the NKBRFSF-China (No 2000048001).

#### References

- [1] J.H. Fendler, *Nanoparticles and Nanostructured Films* (WILEY-VCH, Weinheim 1998).
- [2] J.C. Vartuli, S.S. Shih, C.T. Kresge and J.S. Beck, *Mesopor. Mol. Sieves* 117 (1998) 13.
- [3] C.E. Fowler, D. Khushalani, B. Lebeau and S. Mann, *Adv. Mater.* 13 (2001) 649.
- [4] S. Sadasivan, C.E. Fowler, D. Khushalani, B. Lebeau and S. Mann, *Angew. Chem., Int. Ed.* 41 (2002) 2151.
- [5] S. Sadasivan, D. Khushalani, B. Lebeau and S. Mann, *J. Mater. Chem.* 13 (2003) 1023.
- [6] J. Lee, J. Kim and T. Hyeon, *Chem. Commun.* (2003) 1138.
- [7] Y. Liu and T.J. Pinnavaia, *J. Am. Chem. Soc.* 125 (2003) 2376.
- [8] N. Yao, G.X. Xiong, S.S. Shen, M.Y. He, W.S. Yang and X.H. Bao, *Catal. Lett.* 78 (2002) 37.
- [9] S.R. Zhai, W. Wei, D. Wu and Y.H. Sun, *Catal. Lett.* 89 (2003) 261.
- [10] S.A. Bagshaw, in: *Mesoporous Molecular Sieves 1998, Studies in Surface Science and Catalysis*, Vol. 117, eds. L. Bonneviot, F. Beland, S. Giasson and S. Kaliaguine (Elsevier, Amsterdam, 1998), p. 381.
- [11] J.M. Kim, C.H. Ko, C.H. Shin and R. Ryoo, *J. Phys. Chem.* 99 (1995) 16742.
- [12] S. Biz and M.G. White, *J. Phys. Chem. B* 103 (1999) 8432.
- [13] M.T. Janicke, C.C. Landry, S.C. Christiansen, S. Birtalan, G.D. Stucky and B.F. Chmelka, *Chem. Mater.* 11 (1999) 1342.
- [14] A. Corma, V. Fornes, M.T. Navarro and J. Perez-Pariente, *J. Catal.* 148 (1994) 569.
- [15] J. Aguado, K.P. Serrano and J.M. Escola, *Micropor. Mesopor. Mater.* 34 (2000) 43.
- [16] X.S. Zhao, M.G.Q. Lu and C. Song, *J. Mol. Catal. A* 191 (2003) 67.
- [17] M. Niwa, N. Katada, M. Sawa and Y. Murakami, *J. Phys. Chem.* 99 (1995) 8812.
- [18] D.Y. Zhao, C. Nie, Y.M. Zhou, S.J. Xie, L.M. Huang and Q.Z. Li, *Catal. Today* 68 (2001) 11.
- [19] H. Koch and W. Reschetilowski, *Micropor. Mesopor. Mater.* 25 (1998) 127.
- [20] R. Mokaya, *J. Catal.* 186 (1999) 470.
- [21] S.S. Kim, T.R. Pauly and T.J. Pinnavaia, *Chem. Commun.* (2000) 835.